Oxidative Addition of the Ethane C—C Bond to Pd. An *ab Initio* Benchmark and DFT Validation Study

G. THEODOOR DE JONG,[1] DAAN P. GEERKE,[1] AXEL DIEFENBACH,[2],* MIQUEL SOLÀ,[3] F. MATTHIAS BICKELHAUPT[1]

[1]*Afdeling Theoretische Chemie, Scheikundig Laboratorium der Vrije Universiteit, De Boelelaan 1083, NL-1081 HV Amsterdam, The Netherlands*

[2]*Fachbereich Chemie der Philipps-Universität Marburg, Hans-Meerwein-Straße, D-35032 Marburg, Germany*

[3]*Institut de Química Computacional, Universitat de Girona, Campus Montilivi, E-17071 Girona, Catalonia, Spain*

Received 3 January 2005; Accepted 7 March 2005
DOI 10.1002/jcc.20233
Published online in Wiley InterScience (www.interscience.wiley.com).

Abstract: We have computed a state-of-the-art benchmark potential energy surface (PES) for the archetypal oxidative addition of the ethane C—C bond to the palladium atom and have used this to evaluate the performance of 24 popular density functionals, covering LDA, GGA, meta-GGA, and hybrid density functionals, for describing this reaction. The *ab initio* benchmark is obtained by exploring the PES using a hierarchical series of *ab initio* methods [HF, MP2, CCSD, CCSD(T)] in combination with a hierarchical series of five Gaussian-type basis sets, up to *g* polarization. Relativistic effects are taken into account either through a relativistic effective core potential for palladium or through a full four-component all-electron approach. Our best estimate of kinetic and thermodynamic parameters is −10.8 (−11.3) kcal/mol for the formation of the reactant complex, 19.4 (17.1) kcal/mol for the activation energy relative to the separate reactants, and −4.5 (−6.8) kcal/mol for the reaction energy (zero-point vibrational energy-corrected values in parentheses). Our work highlights the importance of sufficient higher angular momentum polarization functions for correctly describing metal-*d*-electron correlation. Best overall agreement with our *ab initio* benchmark is obtained by functionals from all three categories, GGA, meta-GGA, and hybrid DFT, with mean absolute errors of 1.5 to 2.5 kcal/mol and errors in activation energies ranging from −0.2 to −3.2 kcal/mol. Interestingly, the well-known BLYP functional compares very reasonably with a slight underestimation of the overall barrier by −0.9 kcal/mol. For comparison, with B3LYP we arrive at an overestimation of the overall barrier by 5.8 kcal/mol. On the other hand, B3LYP performs excellently for the central barrier (i.e., relative to the reactant complex) which it underestimates by only −0.1 kcal/mol.

 J Comput Chem 26: 1006–1020, 2005

Key words: *ab initio* benchmark; activation of C—C bond; basis sets; catalysis; density functional validation; palladium; relativistic four-component calculations

Introduction

Alkanes, the "noble gases of organic chemistry," are rather inert chemical substances, which is reflected in their trivial name, paraffins, from the Latin *parum affinis* (without affinity).[1] The activation of the C—H or C—C bonds of alkanes is one of the great challenges in organic chemistry and catalysis, as it is often the first step in the catalytic conversion of the abundant but nonreactive alkanes into more useful products.[2,3] In the group of the transition metal elements, palladium is one of the most important catalysts, mostly in conjunction with ligands.[4] The insertion of the palladium atom into C—H and C—C bonds in alkanes has therefore received considerable attention, both experimentally[5–9] and theoretically.[6,8,10–23] Recently, we have investigated the insertion of the Pd-d^{10} atom into the C—H bond of methane as an important example of this type of

*Present address: SerCon GmbH

Correspondence to: F. M. Bickelhaupt; e-mail: FM.Bickelhaupt@few.vu.nl

Contract/grant sponsor: The Netherlands Organization for Scientific Research (NWO-CW and NWO-NCF)

This article includes Supplementary Material available from the authors upon request or via the Internet at http://www.interscience.wiley.com/jpages/0192-8651/suppmat

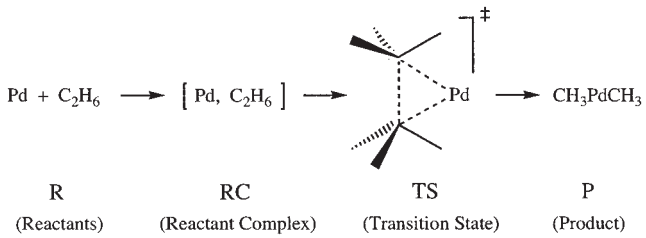

CHART 1. Model reaction and nomenclature.

reactions.[24,25] Among others, we have demonstrated the importance of taking into account sufficient higher angular momentum polarization functions, *f* and *g*, for correctly describing metal-*d*-electron correlation and, thus, for obtaining reliable relative energies.[24] Furthermore, it was shown that density functional theory[26–28] (DFT) is able to reproduce the best *ab initio* (coupled-cluster) results within 1 to 2 kcal/mol.[25] A systematic comparison of functionals revealed that the well-known BLYP functional still performs as one of the best functionals, even better than most of the high-level meta-GGA and hybrid functionals. In this work, we extend our investigations to the oxidative addition of the ethane C—C bond to the Pd-d^{10} atom (see Chart 1). This reaction is archetypal for the activation of C—C single bonds in alkanes. At the same time, it constitutes the reverse reaction of the important class of C—C coupling through reductive elimination, which is therefore also covered.

Experimental investigations on the kinetics of the reaction of palladium with alkanes have been carried out by Weisshaar and coworkers[7,8] using laser-induced fluorescence techniques, and more recently, by Campbell, specifically for palladium and methane.[9] These studies show that Pd forms collisionally stabilized complexes with alkanes and that the rate of conversion of the educts is very small. The exponential decay of the Pd signal vs. alkane pressure suggests a complexation energy of at least 8 kcal/mol for Pd–alkane complexes.[7] This provides us with an experimental boundary condition for the stability of the reactant complex of Pd + ethane.

The purpose of the present study is twofold. In the first place, we wish to obtain a reliable benchmark for the potential energy surface (PES) for the oxidative addition of the C—C bond of ethane to Pd(0). This is done by exploring this PES with a hierarchical series of *ab initio* methods {Hartree–Fock (HF), second-order Møller–Plesset perturbation theory (MP2),[29] and coupled cluster theory[30] with single and double excitations (CCSD),[31] and with triple excitations treated perturbatively [CCSD(T)][32]} in combination with a hierarchical series of Gaussian-type basis sets of increasing flexibility and polarization (up to *g* functions). The basis set superposition error (BSSE) is accounted for by counterpoise correction (CPC).[33] Relativistic effects are treated with a full four-component all-electron approach. The existing computational benchmark for oxidative addition of ethane to palladium was obtained by Blomberg and coworkers[8] with the parameterized configuration interaction method PCI-80, in which the effect of correlation is estimated by an extrapolation procedure.[34] The PCI-80 study arrives at a Pd + ethane complexation energy of 6.6 kcal/mol, an activation energy of 19.5 kcal/mol and a reaction energy of 5.5 kcal/mol (see Table 1).

These values and, in particular, the activation energies appear to be rather sensitive to the level of theory used. The activation energy ranges from 38.6 to 12.5 kcal/mol (see Table 1). In view of

Table 1. Literature Values for Relative Energies (in kcal/mol) of the Stationary Points along the Reaction Coordinate for the Oxidative Insertion of Pd into the C—C Bond of C_2H_6.

		Basis set quality[a]				
Reference	Method	Pd	C and H	RC	TS	P
10, 11	GVB-RCI//HF	DZP[b]	DZ		38.6	16.0
12	CCI+Q//CASSCF	TZP[c]	DZP		39.2	19.7
12	CCI+Q//CASSCF	TZP+2*f*[d]	TZP		31.5	7.5
15	CCSD(T)//HF	TZP+3*f*[e]	TZP		23.1	−0.2
8	PCI-80//HF	TZP+*f*[f]	DZP	−6.6[h]	19.5[h]	−5.5[h]
19	BP86	TZP[g]	TZ2P[g]	−10.5	12.5	−11.8

[a]Main characteristics of the basis set used in the higher level single-point calculations. For Pd, DZP is double-ζ for valence 4*d* shell with one set of polarization functions for 5*p* shell; TZP is triple-ζ for valence 4*d* shell with one set of polarization functions for 5*p* shell. For C and H, DZP is double-ζ with one set of polarization functions, 3*d* for C and 2*p* for H; TZP is triple-ζ with one set of polarization functions, 3*d* for C and 2*p* for H; TZ2P is triple-ζ with two sets of polarization functions, 3*d* and 4*f* for C, and 2*p* and 3*d* for H.
[b]ECP for [Kr] core; valence electrons: (3*s*3*p*3*d*)/[3*s*2*p*2*d*] (ref. 99).
[c]Augmented Huzinaga basis (ref. 100), Raffenetti contraction scheme (ref. 101): (17*s*13*p*9*d*)/[8*s*7*p*4*d*].
[d]Same as c but with larger primitive and contracted basis: (17*s*13*p*10*d*4*f*)/[8*s*7*p*5*d*2*f*].
[e]Same as c but with larger primitive and contracted basis: (17*s*13*p*9*d*3*f*)/[7*s*6*p*4*d*3*f*].
[f]Same as e but with three *f* functions contracted: (17*s*13*p*9*d*3*f*)/[7*s*6*p*4*d*1*f*].
[g]Slater-type orbitals.
[h]With ZPE correction.

this situation, it is appropriate to explore to what extent the PCI-80 values are converged with respect to both the order of correlation incorporated into the theoretical method and the degree of flexibility and polarization of the basis set.

The second purpose of our work is to evaluate the performance of 24 popular density functionals, covering LDA, GGA, meta-GGA, and hybrid density functionals, for describing the oxidative addition of the ethane C—C bond to Pd, using our new *ab initio* benchmark as reference point. Here, we anticipate that although the latter turns out to be satisfactory in terms of accuracy and reliability, it is prohibitively expensive if one wishes to study more realistic model catalysts and substrates. Thus, our survey of 24 density functionals serves to validate one or more of these DFT approaches as a computationally more efficient alternative to high-level *ab initio* theory in future investigations in the field of computational catalysis.[35] A general concern, however, associated with the application of DFT to the investigation of chemical reactions is its notorious tendency to underestimate activation energies.[19,36–41] Furthermore, we investigate the dependence of the resulting PES on the basis-set size and on the use of the frozen-core approximation. Thus, we arrive at a ranking of density functional approaches in terms of the accuracy with which they describe the PES of our model reaction, in particular the activation energy. We focus on the overall activation energy, that is, the difference in energy between the TS and the separate reactants, which is decisive for the rate of chemical reactions in the gas phase, in particular, if they occur under low-pressure conditions in which the reaction system is (in good approximation) thermally isolated[7,42] (see also Section II of ref. 43). But we also address the central barrier, that is, the difference in energy between the TS and the reactant complex. Here, we anticipate that, in line with previous work on palladium-induced C—H activation in methane,[25] the well-known BLYP GGA functional is found to perform very satisfactorily, in fact, as good as the much advocated B3LYP hybrid functional.

Method and Computational Details

Geometries

All geometry optimizations have been done with DFT using the Amsterdam Density Functional (ADF) program.[44–47] For seven different GGA-functionals, the performance for computing the geometries and relative energies of the stationary points along the PES of our model reaction (see Chart 1) was compared. These density functionals are BP86,[48,49] BLYP,[48,50] PW91,[51–54] PBE,[55,56] revPBE,[57] RPBE[58] and OLYP.[50,59] They were used in combination with the TZ2P basis set, which is a large uncontracted set of Slater-type orbitals (STOs) containing diffuse functions, which is of triple-ζ quality and has been augmented with two sets of polarization functions: 2*p* and 3*d* on H, 3*d* and 4*f* on C, 5*p* and 4*f* on Pd. The core shells of carbon (1*s*) and palladium (1*s*2*s*2*p*3*s*3*p*3*d*) were treated by the frozen-core approximation.[44] An auxiliary set of *s*, *p*, *d*, *f* and *g* STOs was used to fit the molecular density and to represent the Coulomb and exchange potentials accurately in each SCF cycle.[44] Relativistic effects were accounted for using the zeroth-order regular approximation (ZORA).[60] For each of the seven GGAs, all stationary points were confirmed to be equilibrium structures (no imaginary frequencies) or a transition state (one imaginary frequency) through vibrational analysis. Enthalpies at 298.15 K and 1 atmosphere were calculated from 0 K electronic energies according to the following equation, assuming an ideal gas:

$$\Delta H_{298} = \Delta E + \Delta E_{\mathrm{trans},298} + \Delta E_{\mathrm{rot},298} + \Delta E_{\mathrm{vib},0} + \Delta(\Delta E_{\mathrm{vib},0})_{298} + \Delta(pV) \quad (1)$$

Here, $\Delta E_{\mathrm{trans},298}$, $\Delta E_{\mathrm{rot},298}$, and $\Delta E_{\mathrm{vib},0}$ are the differences between products and reactants in translational, rotational, and zero-point vibrational energy, respectively; $\Delta(\Delta E_{\mathrm{vib},0})_{298}$ is the change in the vibrational energy difference going from 0 to 298.15 K. The vibrational energy corrections are based on our frequency calculations. The molar work term $\Delta(pV)$ is $(\Delta n)RT$; $\Delta n = -1$ for two reactants (Pd + C_2H_6) combining to one species. Thermal corrections for the electronic energy are neglected.

Table 2. Basis Sets Used in the *Ab Initio* Calculations with DIRAC.

Name	Pd	C and H
BS1	$(24s16p13d)^a$	cc-aug-pVDZ[b]
BS2	$(24s16p13d)^a + 1f$	cc-aug-pVDZ[b]
BS3	$(24s16p13d)^a + 4f$	cc-aug-pVDZ[b]
BS4	$(24s16p13d)^a + 4f + p$	cc-aug-pVDZ[b]
BS5	$(24s16p13d)^a + 4f + p + g$	cc-aug-pVDZ[b]

[a]TZP quality.
[b]Completely uncontracted.

Ab Initio *Calculations*

Based on the ZORA-BLYP/TZ2P geometries, energies of the stationary points were computed in a series of single-point calculations with the program package DIRAC[61,62] using the following hierarchy of quantum chemical methods: HF, MP2, CCSD, and CCSD(T). Relativistic effects are accounted for using a full all-electron four-component Dirac–Coulomb approach with a spin-free Hamiltonian (SFDC).[63] The two-electron integrals over exclusively the small components have been neglected and corrected with a simple Coulombic correction, which has been shown reliable.[64]

A hierarchical series of Gaussian-type basis sets was used (see Table 2). For carbon and hydrogen Dunning's correlation consistent augmented double-ζ (cc-aug-pVDZ) basis set was used.[65,66] This was used in uncontracted form because it is technically difficult to use contracted basis sets in the kinetic balance procedure in DIRAC.[67] The basis set of palladium is based on an uncontracted basis set (24*s*16*p*13*d*), which is of triple-ζ quality, and has been developed by Faegri (personal communication). The combination of this basis set for palladium and the afore-mentioned basis sets for carbon and hydrogen is denoted BS1 (see Table 2). As a first extension, in BS2, one set of 4*f* polarization functions was added with an exponent of 1.472, as reported by Ehlers et al.[68] In BS3, this single set of 4*f* functions was substituted by four sets of 4*f* polarization functions as reported by Langhoff

and coworkers with exponents 3.611217, 1.29541, 0.55471, and 0.23753.[69] Thereafter, going to BS4, an additional set of diffuse *p* functions was introduced with exponent 0.141196, as proposed by Osanai et al.[70] Finally, the largest basis set of the series, BS5, was created by adding a set of *g* functions, with an exponent of 1.031690071. This value is close to but not exactly equal to the exponent of the *g* functions optimized by Osanai. Instead it is equal to the value of one of the exponents of the *d* set of Faegri, which reduces computational costs.

We wish to point out that the basis sets BS1–BS5 used in the present study (see Table 2) differ from those, B1– B6, used in our recent study on the oxidative addition of methane to Pd (see Table II in ref. 24). BS1 and BS2 are exactly equal to B1 and B2. However, from B2 to B3, the carbon and hydrogen basis sets in ref. 24 (CH_4 + Pd) are extended from uncontracted cc-aug-pVDZ to uncontracted cc-aug-pVTZ. This was not possible for the present, larger model system (C_2H_6 + Pd), as it causes the required memory to exceed our available allotment. Therefore, in the present study, we used exclusively uncontracted cc-aug-pVDZ for carbon and hydrogen. Note, however, that regarding palladium BS2–BS5 corresponds with B3–B6 of ref. 24. We have tested how the results of ref. 24 are affected if the present approach for C_2H_6 + Pd (i.e., BS1–BS5 instead of B1–B6) is used also for CH_4 + Pd. At the highest level of theory, namely, counterpoise-corrected CCSD(T)/BS5, the energy of formation of the reactant complex of CH_4 + Pd is −7.0 kcal/mol, the activation barrier is 6.9 kcal/mol and the reaction energy amounts to 1.7 kcal/mol. These relative energies are consistently ca. 1 kcal/mol higher than and, thus, compare reasonably well with the corresponding counterpoise-corrected CCSD(T)/B6 values of ref. 24, which are −8.1, 5.8, and 0.8 kcal/mol.

DFT Calculations

Based on the ZORA-BLYP/TZ2P geometries, we have also evaluated in a series of single-point calculations the dependence of the ZORA-BLYP relative energies of stationary points along the PES on the basis-set size for four different all-electron (i.e., no frozen-core approximation) STO basis sets, namely ae-DZ, ae-TZP, ae-TZ2P, and ae-QZ4P, and on the use of the frozen-core approximation. The ae-DZ basis set is of double-ζ quality, is unpolarized for C and H but has been augmented with a set of 5*p* polarization functions for Pd. The ae-TZP basis set is of triple-ζ quality and has been augmented with one set of polarization functions on every atom: 2*p* on H, 3*d* on C, and 5*p* on Pd. The ae-TZ2P basis set (the all-electron counterpart corresponding to the above-mentioned TZ2P basis that is used in conjunction with the frozen-core approximation) is also of triple-ζ quality and has been augmented with two sets of polarization functions on each atom: 2*p* and 3*d* on H, 3*d* and 4*f* on C, and 5*p* and 4*f* on Pd. The ae-QZ4P basis set is of quadruple-ζ quality and has been augmented with four sets of polarization functions on each atom: two 2*p* and two 3*d* sets on H, two 3*d* and two 4*f* sets on C, and two 5*p* and two 4*f* sets on Pd.

Finally, based again on the ZORA-BLYP/TZ2P geometries, we have computed in a post-SCF manner, that is, using in all cases the electron density obtained at ZORA-BLYP/ae-TZ2P, the relative energies of stationary points along the PES for various LDA, GGAs, meta-GGAs, and hybrid functionals. In addition to the ones used in the geometry optimizations (see subsection Geometries in this section), the following density functionals were examined: the LDA functional VWN;[71] the GGA-functionals Becke 88x + BR89c,[72,73] FT97,[74] HCTH/93,[75] BOP,[72,76] HCTH/120,[77] HCTH/147,[77] and HCTH/407;[78] the meta-GGA functionals BLAP3,[79] VS98,[80] KCIS,[81] PKZB,[82,83] Bm τ1,[84] OLAP3[59,79] and TPSS;[85,86] and the hybrid functionals B3LYP[87,88] (based on VWN5[89]) and TPSSh.[85,86]

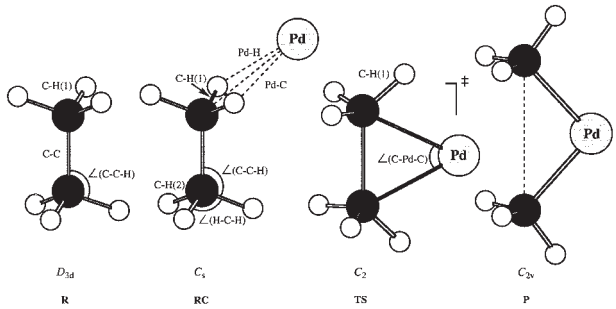

Figure 1. Structures and point group symmetries of the stationary points along the reaction coordinate for the oxidative insertion of Pd into the C—C bond of C_2H_6. See Table 3 for values of geometry parameters.

Results and Discussion

Geometries of Stationary Points

First, we examine the geometries of stationary points along the reaction coordinate of the oxidative insertion of Pd into the C—C bond of ethane, computed with the GGA functionals BP86, BLYP, PW91, PBE, revPBE, RPBE, and OLYP in combination with the TZ2P basis set, the frozen-core approximation, and the zeroth-order regular approximation (ZORA) to account for relativistic effects. Geometry parameters are defined in Figure 1 and their values optimized with each of the seven GGA functionals are collected in Table 3. For each of the functionals, the reaction proceeds from the reactants via formation of a stable reactant complex of C_s symmetry, in which one of the methyl-groups of ethane coordinates in an η^2 fashion to Pd, followed by the transition state of C_2 symmetry and, finally, a stable product of C_{2v} symmetry. All species have been verified through a vibrational analysis to represent equilibrium structures (no imaginary frequencies) or a transition state (one imaginary frequency). The imaginary frequency in the transition state associated with the normal mode that connects reactant complex and product varies, depending on the functional, between 487 and 493 i cm^{-1} (for BP86, BLYP, PW91, PBE, revPBE, RPBE, and OLYP it amounts to 490, 493, 493, 488, 488, 487, and 490 i cm^{-1}).

The geometries obtained with the various GGA functionals do not show significant mutual discrepancies, and they agree well with an earlier DFT study (see Table 3 and Fig. 1).[19] The C—H bond distance values are very robust with respect to changing the functional, with variations in the order of a few thousandths of an angstrom. Note that variations in the length of the activated C—C

Table 3. Geometry Parameters[a] (in Å, Degrees), Optimized with Seven Different Density Functionals and the TZ2P Basis Set with Frozen-Core Approximation,[b] of the Stationary Points along the Reaction Coordinate for the Oxidative Insertion of Pd into the C—C Bond of C_2H_6.

Method		C—H(1)	C—H(2)	C—C	Pd—C	Pd—H	∠(C—C—H)	∠(H—C—H)	∠(C—Pd—C)
BP86	R	1.099		1.532			111.4		
	RC	1.137	1.099	1.532	2.313	1.941	111.3	107.8	
	TS	1.133	1.091	1.927	2.111	2.059	133.8	107.7	54.3
	P	1.104	1.096	2.960	1.998	2.491	145.2	110.7	95.6
BLYP	R	1.098		1.541			111.3		
	RC	1.126	1.098	1.541	2.418	2.023	111.3	107.9	
	TS	1.123	1.089	1.945	2.167	2.102	133.2	108.7	53.3
	P	1.101	1.094	3.028	2.025	2.513	144.6	111.0	96.7
PW91	R	1.097		1.529			111.4		
	RC	1.136	1.098	1.528	2.311	1.941	111.3	107.8	
	TS	1.130	1.090	1.926	2.107	2.063	134.0	107.9	54.4
	P	1.102	1.095	2.932	1.995	2.491	146.0	110.7	94.6
PBE	R	1.099		1.530			111.4		
	RC	1.138	1.099	1.530	2.308	1.940	111.3	107.8	
	TS	1.133	1.092	1.928	2.105	2.066	134.1	107.8	54.5
	P	1.104	1.097	2.937	1.996	2.492	145.9	110.7	94.8
revPBE	R	1.100		1.537			111.4		
	RC	1.133	1.100	1.537	2.374	1.988	111.4	107.8	
	TS	1.131	1.093	1.933	2.127	2.088	134.0	108.1	54.1
	P	1.105	1.097	2.971	2.008	2.504	145.5	110.6	95.4
RPBE	R	1.100		1.538			111.4		
	RC	1.131	1.101	1.539	2.396	2.005	111.4	107.8	
	TS	1.130	1.093	1.935	2.133	2.093	134.1	108.1	54.0
	P	1.105	1.098	2.976	2.012	2.508	145.6	110.6	95.4
OLYP	R	1.096		1.529			111.4		
	RC	1.122	1.096	1.530	2.426	2.027	111.6	107.7	
	TS	1.124	1.089	1.932	2.109	2.090	134.7	108.0	54.5
	P	1.100	1.093	2.961	1.997	2.492	145.4	110.5	95.7

[a]See Figure 1 for definition.
[b]Relativistic effects treated with ZORA (see Method section).

bond become larger, up to 0.09 Å in the product, as the reaction progresses. This is in line with the fact that this bond is being broken along the reaction coordinate, which causes the PES to become increasingly soft in this coordinate and, thus, sensitive to changes in the computational method. More pronounced variations are found for the weak Pd—C and Pd—H bonds. This holds especially for the loosely bound reactant complex, which shows fluctuations of up to one tenth of an angstrom for Pd—C and in the order of hundredths for Pd—H. The variations in these bond distances drop to a few hundredths or even a few thousandths of an angstrom as the reaction proceeds to transition state and product in which more stable coordination bonds are formed. Thus, only moderate (although not negligible) variations in bond distances occur along the various functionals and they are more pronounced for the softer (or broken) bonds. This is, of course, also reflected by the variations in bond angles. These variations are very small as firmly bound triplets of atoms are involved, but can become somewhat larger for angles opposite to a soft bond (e.g., up to 2° for the C—Pd—C angle).

Thus, the various functionals yield essentially the same geometries. Later on, in the section Validation of DFT, we show that BLYP also performs excellently in terms of relative energies of stationary points. Based on these findings, and the fact that BLYP is robust and well established, we choose the geometries of this functional, that is, ZORA-BLYP/TZ2P, to compute an *ab initio* benchmark potential energy surface in the next section.

Benchmark Energies from **Ab Initio** *Calculations*

As pointed out in the introduction, the relative energies of stationary points along the reaction profile of Pd insertion into the ethane C—C bond, especially the activation energy, appear to be highly sensitive to the level of theory used, as witnessed by the large spread in values computed earlier (see Table 1). Here, we report the first systematic investigation of the extent to which these values are converged at the highest level of theory used. This survey is based on geometries of stationary points that were optimized at the ZORA-BLYP/TZ2P level of relativistic DFT (see preceding section and Table 3). The results of our *ab initio* computations are collected in Tables 4 and 5 (relative energies and BSSE) and graphically displayed in Figure 2 (reaction profiles). Table S1 in the supplementary material shows the total energies in a.u. of all species occurring at the stationary points as well as the total energies of the corresponding Pd and ethane fragments, with

Table 4. Relative Energies (in kcal/mol) of the Stationary Points along the Reaction Coordinate for Oxidative Insertion of Pd into the C—C Bond of C_2H_6, without (no CPC) and with Counterpoise Correction (with CPC), Computed at Several Levels of *Ab Initio* Theory.

		RC		TS		P	
Method	Basis set	no CPC	with CPC	no CPC	with CPC	no CPC	with CPC
HF	BS1	5.0	5.5	57.4	58.0	40.8	41.2
	BS2	4.8	5.3	57.0	57.6	38.7	39.0
	BS3	4.6	5.2	56.3	57.0	36.8	37.2
	BS4	4.7	5.2	56.3	57.1	36.8	37.2
	BS5	4.6	5.1	56.2	56.9	36.2	36.6
MP2	BS1	−11.5	−6.4	17.5	25.2	−5.0	4.8
	BS2	−16.6	−9.1	8.1	19.0	−16.8	−2.9
	BS3	−15.4	−12.3	8.5	13.3	−11.4	−5.7
	BS4	−14.3	−12.5	9.6	13.1	−10.4	−6.0
	BS5	−14.8	−13.0	8.5	11.9	−10.5	−6.3
CCSD	BS1	−9.7	−4.5	25.0	32.7	−0.1	9.1
	BS2	−12.5	−5.9	20.5	30.0	−6.2	5.5
	BS3	−10.4	−7.7	23.0	27.1	−1.6	3.0
	BS4	−9.6	−8.0	23.8	26.9	−0.9	2.7
	BS5	−9.6	−8.1	23.6	26.6	−0.4	2.9
CCSD(T)	BS1	−12.5	−5.9	18.4	27.7	−6.5	4.7
	BS2	−16.0	−8.0	12.4	23.7	−14.7	−0.9
	BS3	−14.0	−10.2	14.9	20.4	−9.9	−3.9
	BS4	−12.4	−10.5	16.5	20.1	−8.3	−4.3
	BS5	−12.5	−10.8	16.1	19.4	−8.2	−4.5

Table 5. Basis Set Superposition Error (BSSE, in kcal/mol) for Pd and C_2H_6 in the Stationary Points along the Reaction Coordinate for Oxidative Insertion of Pd into the C—C Bond of C_2H_6, Computed at Several Levels of *Ab Initio* Theory.

		RC			TS			P		
Method	Basis set	Pd	C_2H_6	Total	Pd	C_2H_6	Total	Pd	C_2H_6	Total
HF	BS1	0.5	0.0	0.5	0.5	0.1	0.6	0.2	0.2	0.3
	BS2	0.5	0.0	0.5	0.5	0.1	0.6	0.2	0.2	0.3
	BS3	0.5	0.1	0.5	0.5	0.2	0.7	0.2	0.3	0.4
	BS4	0.4	0.1	0.5	0.4	0.3	0.7	0.1	0.3	0.4
	BS5	0.4	0.1	0.5	0.4	0.3	0.7	0.1	0.3	0.4
MP2	BS1	4.9	0.3	5.2	6.9	0.8	7.7	8.2	1.6	9.7
	BS2	7.2	0.3	7.5	10.2	0.8	10.9	12.3	1.6	13.9
	BS3	2.7	0.5	3.2	3.3	1.5	4.7	3.3	2.4	5.7
	BS4	1.2	0.6	1.8	1.7	1.8	3.4	1.7	2.6	4.3
	BS5	1.1	0.6	1.7	1.5	1.8	3.4	1.5	2.7	4.2
CCSD	BS1	5.0	0.3	5.3	6.9	0.7	7.6	8.1	1.2	9.2
	BS2	6.3	0.3	6.6	8.8	0.7	9.5	10.5	1.2	11.7
	BS3	2.3	0.4	2.7	2.7	1.4	4.1	2.8	1.8	4.6
	BS4	1.0	0.6	1.6	1.5	1.6	3.1	1.5	2.0	3.5
	BS5	1.0	0.6	1.5	1.3	1.7	3.0	1.2	2.1	3.3
CCSD(T)	BS1	6.2	0.3	6.6	8.6	0.8	9.3	9.9	1.2	11.2
	BS2	7.7	0.3	8.0	10.6	0.8	11.4	12.6	1.3	13.8
	BS3	3.3	0.5	3.8	4.0	1.5	5.5	4.1	2.0	6.1
	BS4	1.2	0.6	1.8	1.7	1.8	3.5	1.8	2.1	4.0
	BS5	1.1	0.6	1.7	1.5	1.8	3.4	1.5	2.2	3.7

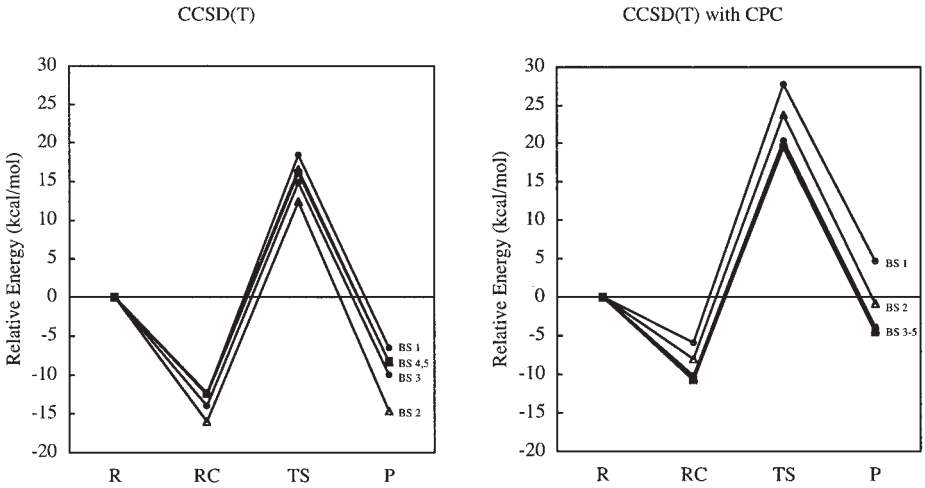

Figure 2. Reaction profile for the oxidative insertion of Pd into the C—C bond of C_2H_6, computed with CCSD(T) for various basis sets, without (left panel) and with counterpoise correction (right panel). Based on geometries optimized at ZORA-BLYP/TZ2P (i.e., using the frozen-core approximation).

and without the presence of the other fragment as ghost. In this way, we can calculate the BSSE and carry out a counterpoise correction (CPC).

We proceed with examining the reaction profiles for the oxidative insertion of Pd into the ethane C—C bond, that is, the energies of the stationary points relative to the reactants Pd and ethane, which are collected in Table 4 and, for CCSD(T), displayed in Figure 2. At all levels of theory except Hartree–Fock, the reaction profiles are characterized by the formation of a stable reactant complex (RC), which leads via the transition state for insertion (TS) to the oxidative addition product (P). Three striking observations can be made: (1) the spread in values of computed relative energies, depending on the level of theory and basis set, is enormous, up to nearly 60 kcal/mol; (2) the size of the BSSE is also remarkably large, up to ca. 14 kcal/mol; (3) convergence with basis-set size of the computed energies is still not reached with standard basis sets used routinely in CCSD(T) computations on organometallic and coordination compounds. The lack of any correlation leads to a complete failure at the HF level, which yields an unbound RC and a strongly exaggerated activation barrier of ca. 57 kcal/mol. The failure of HF for describing the PES of our model reaction is not unexpected because electron correlation, which is not contained in this approach, is important.[90,91] The activation energy drops significantly when electron correlation is introduced. Along HF, CCSD and CCSD(T) in combination with basis set BS1, for example, the activation barrier decreases from 57.4 to 25.0 to 18.4 kcal/mol. But also the correlated CCSD(T) values obtained with basis sets BS1 up to BS3, comparable in quality to standard basis sets such as LANL2DZ[92,93] without or with up to four *f* functions added, are questionable, as they are obviously not converged as a function of the basis-set size. [Indeed, preliminary calculations with the program Gaussian[94] at CCSD(T) with basis sets cc-aug-pVDZ for C and H, and LANL2DZ (−13.0, 16.2, and −4.7 kcal/mol for RC, TS, and P) and LANL2DZ+*f* (−17.6, 8.7, and −14.1 kcal/mol for RC, TS, and P), respectively, for Pd yield similar trends in PES as the calculations with the program DIRAC at CCSD(T) with basis sets BS1 and BS2, respectively (see Table 4).] For example, the activation energy of 18.4 kcal/mol at CCSD(T)/BS1 agrees remarkably well with the PCI-80 value of 19.5 kcal/mol obtained by Siegbahn and coworkers (see Table 1). This agreement is, however, fortuitous. The activation energy computed at CCSD(T) drops further from 18.4 kcal/mol for basis set BS1 to 12.4 kcal/mol for basis set BS2 in which one *f* polarization function has been added. Thereafter, along BS2 to BS5, the activation energy increases again, although not monotonically, from 12.4 to 16.1 kcal/mol, as three more sets of *f* functions, an additional set of diffuse *p* functions and a set of *g* functions are added to the basis set of Pd (see Tables 2 and 4). This is illustrated by Figure 2, left diagram, which shows the CCSD(T) reaction profiles and how they vary along basis sets BS1–BS5.

Next, we note that the BSSE takes on large values in the correlated *ab initio* methods, whereas it is negligible if correlation is completely neglected, that is, in HF (see Table 5). The BSSE increases somewhat going from BS1 to BS2, and decreases from BS2 to BS5. At the CCSD(T) level, for example, the BSSE for the TS of the reaction amounts to 9.3, 11.4, 5.5, 3.5, and 3.4 kcal/mol along the basis sets BS1 to BS5, whereas the corresponding BSSE values at HF are only ca. 0.7 kcal/mol (Table 5). The BSSE increases along the reaction coordinate, that is, going from RC to TS to P. The reason for this is that along this series of stationary points, the carbon and hydrogen atoms and, thus, their basis functions come closer too and begin to surround the palladium atom. This effectively improves the flexibility and polarization of the basis set and thus the description of the wave function in the region of the palladium atom. Note that, for basis sets BS1–BS3, the BSSE stems predominantly from the improvement of the stabilization of palladium as ethane ghost functions are added. This contribution to the BSSE quickly reduces as the basis set of palladium is improved and, for the two largest basis sets, BS4 and BS5 (which contain *g* as well as diffuse *p* functions on Pd) it is

Table 6. Relative Energies without (ΔE) and with Zero-Point Vibrational Energy Correction ($\Delta E + \Delta ZPE$), and Relative Enthalpies at 298.15 K (ΔH) of the Stationary Points[a] along the Reaction Coordinate for Oxidative Insertion of Pd into the C—C Bond of C_2H_6 (in kcal/mol), Computed with Seven Different Density Functionals and the TZ2P Basis Set with Frozen-Core Approximation,[b] and Compared to *Ab Initio* Benchmarks from This Work and Literature.[c]

	ΔE			$\Delta E + \Delta ZPE$			ΔH		
Method	RC	TS	P	RC	TS	P	RC	TS	P
DFT computations (this work)[b]									
BP86	−11.0	11.3	−13.4	−11.5	8.8	−15.8	−11.9	8.2	−15.7
BLYP	−6.8	18.3	−9.3	−7.2	15.9	−11.5	−7.5	15.4	−11.5
PW91	−12.4	9.7	−14.3	−12.9	7.3	−16.5	−13.3	6.7	−16.5
PBE	−11.9	10.2	−13.5	−12.5	7.7	−15.9	−12.9	7.1	−15.8
revPBE	−6.5	17.3	−7.7	−7.1	14.8	−10.0	−7.3	14.3	−10.0
RPBE	−6.0	18.2	−6.9	−6.5	15.7	−9.3	−6.8	15.2	−9.2
OLYP	−1.3	25.1	0.8	−1.8	22.8	−1.5	−2.0	22.2	−1.5
Ab initio benchmarks (this work and literature)[c]									
CCSD(T)//BLYP	−10.8	19.4	−4.5	−11.3	17.1	−6.8			
PCI-80//HF				−6.6	19.5	−5.5			

[a]Geometries and energies computed at the same level of theory. See Figure 1 for structures.
[b]Relativistic effects treated with ZORA (see Method section).
[c]CCSD(T) benchmark from this work and PCI-80 from ref. 8.

approximately equal to (in fact, slightly smaller than) the extra stabilization of the ethane fragment due to adding palladium ghost functions. Note that the total BSSE at CCSD(T) has been considerably decreased, that is, from 11.4 kcal/mol for BS2 to only 3.4 kcal/mol for BS5 (Table 5) and is thus clearly smaller than the relative energies that we compute, in particular the activation energy of 16.1 kcal/mol, see CCSD(T)/BS5 in Table 4.

The high sensitivity of the PES for oxidative addition of the ethane C—C bond to Pd highlights the prominent role that electron correlation plays in our model systems. It is striking that the relative CCSD(T) energies have still not reached convergence for basis set BS3, which is of a quality comparable to that of standard basis sets such as LANL2DZ,[92] augmented with four *f* polarization functions, for Pd (see Table 4 and Fig. 2, left; see also above). This may be somewhat surprising in view of earlier reports that such basis sets yield satisfactory energies for organometallic and coordination compounds (see, e.g., the excellent reviews by Frenking et al.[90] and by Cundari et al.[91]). On the other hand, it is consistent with the large variation of values for the thermodynamic and kinetic parameters obtained in earlier theoretical studies of the present model reaction (see Table 1). It is also consistent with our findings for the PES for oxidative addition of the methane C—H bond to Pd, which shows exactly the same sensitivity and behavior.[24] One reason for the increased sensitivity that we find towards the quality of the theoretical approach is that the presence of *f* polarization functions is only the minimum requirement for describing the electron correlation of palladium 4*d* electrons. In this respect, the palladium basis sets in BS1, BS2, and BS3 should be considered minimal and cannot be expected to have achieved convergence. Furthermore, the consequences of any inadequacy in the basis set shows up more severely in processes such as ours, which involve a bare, uncoordinated transition metal atom as one of the reactants because here the effect of additional assistance of basis functions on the substrate is more severe than in situations where the transition metal fragment is already surrounded by, for example, ligands. This shows up in the relatively large BSSE values for CCSD(T)/BS1–BS3.

Thus, we have been able to achieve virtual convergence of the CCSD(T) relative energies by using a larger than standard basis set and by correcting for the BSSE through counterpoise correction (see Table 4 and Fig. 2, right panel). Indeed, along BS2–BS5, the BSSE decreases monotonically from 11.4 to 5.5 to 3.5 to 3.4 kcal/mol, and is thus clearly smaller than the relative energies that we compute (see Table 5). This legitimates the use of counterpoise correction (CPC) as a means to correct for the BSSE. The counterpoise-corrected relative energies at CCSD(T) are converged within a few tenths of a kcal/mol. For example, the counterpoise-corrected activation energy at CCSD(T) amounts to 26.6, 27.7, 23.7, 20.4, 20.1, and 19.4 kcal/mol. Our best estimate, obtained at CCSD(T)/BS5 with CPC, for the kinetic and thermodynamic parameters of the oxidative insertion of Pd into the ethane C—C bond is −10.8 kcal/mol for the formation of the reactant complex, 19.4 kcal/mol for the activation energy relative to the separate reactants, and −4.5 kcal/mol for the reaction energy. If we take into account zero-point vibrational energy (ZPE) effects computed at BLYP/TZ2P, this yields −11.3 kcal/mol for the formation of the reactant complex, +17.1 kcal/mol for the activation energy relative to the separate reactants, and −6.8 kcal/mol for the reaction energy (see Table 6). Our benchmark values, in particular the activation energy, agree reasonably well with those obtained by Siegbahn and coworkers at PCI-80,[8] namely, −6.6, +19.5 and −5.5 kcal/mol for RC, TS, and P (see Table 6), and therefore, further consolidate the theoretical reaction profile. They also agree

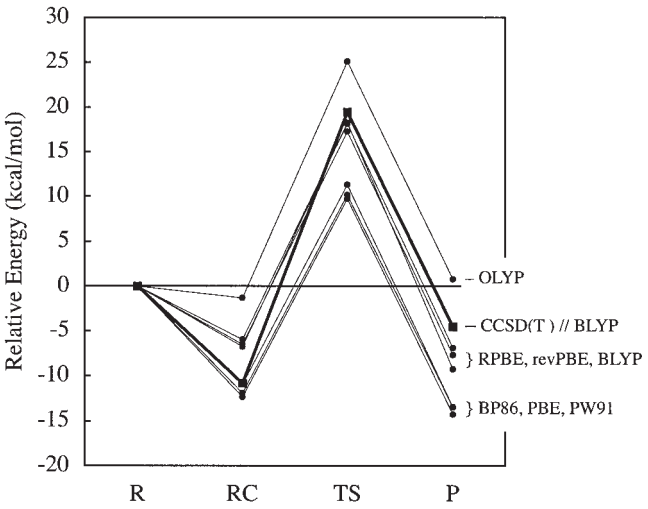

Figure 3. Reaction profile for the oxidative insertion of Pd into the C—C bond of C_2H_6, obtained with seven different GGA density functionals (thin lines) and the TZ2P basis set with frozen-core approximation (geometries and energies computed at the same level of DFT; relativistic effects are treated with ZORA). The counterpoise-corrected CCSD(T) benchmark of this work is also included (thick line).

well, in fact slightly better so than PCI-80, with the experimental result that the reactant complex is bound by at least 8 kcal/mol.[7]

Validation of DFT

Next, we examine the relative energies of stationary points computed with the GGA functionals BP86, BLYP, PW91, PBE, revPBE, RPBE, and OLYP in combination with the TZ2P basis set, the frozen-core approximation, and the zeroth-order regular approximation (ZORA) to account for relativistic effects. Note that for each density functional we use consistently the geometries optimized with that functional, for example, BP86//BP86 or BLYP//BLYP (see section Geometries of Stationary Points). As pointed out in the Introduction, we first focus on the overall activation energy, that is, the difference in energy between the TS and the separate reactants, which is decisive for the rate of chemical reactions in the gas phase, in particular, if they occur under low-pressure conditions. Later on, in the last subsection, we also address the central barrier, that is, the difference in energy between the TS and the reactant complex. Relative energies, with and without zero-point vibrational energy correction, as well as relative enthalpies are collected in Table 6. Relative energies are also graphically represented in Figure 3. The performance of the seven different GGA functionals is assessed by a systematic comparison of the resulting potential energy surfaces with our relativistic four-component CCSD(T) benchmark. For comparison, we have also included in Table 6 the earlier *ab initio* benchmark obtained by Siegbahn and coworkers with the PCI-80 method. It is clear, especially from Figure 3, that the investigated GGAs fall into three groups regarding their agreement with the benchmark results. OLYP clearly underestimates metal–substrate bonding and yields a too weakly bound reactant complex, a barrier that is too high by almost 6 kcal/mol, and an endothermic reaction energy, where it should be exothermic. The situation is opposite for BP86, PBE, and PW91, which seem to overestimate metal–substrate bonding. Although this leads to nice agreement for the reactant complex with the coupled-cluster result, it gives a significantly underestimated barrier (by nearly 10 kcal/mol for PW91) and a too exothermic reaction energy. On the other hand, BLYP and the two revisions of PBE, that is, revPBE and RPBE, achieve quite satisfactory agreement with the coupled-cluster PES, especially for the barrier, which is underestimated by only 1.1 (BLYP), 2.1 (revPBE), and 1.2 kcal/mol (RPBE), with BLYP performing slightly better than the other functionals. Thus, we arrive at the conclusion that we anticipated earlier in the discussion, namely, that BLYP performs excellently for computing relative energies. Furthermore, we notice that here the same order of relative performance of the various GGA functionals emerges as we found in our study on the oxidative addition of the methane C—H bond to Pd, in which BLYP also performed better than other functionals.[25]

We proceed with examining the convergence of the (all-electron) BLYP relative energies of stationary points as the basis set increases along ae-DZ, ae-TZP, ae-TZ2P, and ae-QZ4P, using the ZORA-BLYP/TZ2P geometries, which were also used in the *ab initio* calculations in the preceding section (see Table 3). We also investigate the convergence of the BSSE along this series and the effect of using the frozen-core approximation in the calculations discussed in the preceding paragraph (see also Tables 3 and 5). The results are shown in Table 7 and in Figure 4. In the first place, we note that it is perfectly valid to use the frozen-core approximation as it has hardly any effect on the relative energies. This becomes clear if one compares the frozen-core BLYP/TZ2P results in Table 6 (−6.8, 18.3, and −9.3 kcal/mol for RC, TS, and P) with the corresponding all-electron BLYP/ae-TZ2P data in Table 7 (no CPC: −6.7, 18.5, and −9.5 kcal/mol for RC, TS, and P). The frozen-core and all-electron values of the relative energies agree within 0.2 kcal/mol. Next, the issue of basis set convergence is addressed. The data in Table 7 show that the relative energies of stationary points are already converged to within the order of some tenths of a kcal/mol with the ae-TZ2P basis set. The BSSE drops to 0.5 kcal/mol or less for this basis set and virtually vanishes to less than 0.1 kcal/mol if one goes to ae-QZ4P (see Table 7: the BSSE is the difference between "no CPC" and "with CPC" values). For example, the activation energy without counterpoise correction varies from 23.2 to 19.7 to 18.5 to 18.0 kcal/mol along ae-DZ, ae-TZP, ae-TZ2P, and ae-QZ4P (Table 7, no CPC). The corresponding BSSE amounts to 3.3, 0.3, 0.4, and less than 0.1 kcal/mol (see Table 7). Note that in fact the BSSE is large, that is, a few kcal/mol, only for the smallest, ae-DZ, basis set. This is in line with our previous work on the oxidative addition of CH_4 + Pd, in which we found that basis-set convergence and elimination of the BSSE are achieved much earlier for DFT (i.e., B3LYP) than for correlated *ab initio* methods, for example, CCSD(T).[24] In general, correlated *ab initio* methods depend more strongly on the extent of polarization of the basis set because the polarization functions are essential to generate the configurations through which the wave function can describe the correlation hole. In DFT, on the other hand, the correlation hole is built into the potential and the energy functional and polarization functions mainly play the

Table 7. Relative Energies (in kcal/mol) of the Stationary Points[a] along the Reaction Coordinate for Oxidative Insertion of Pd into the C—C Bond of C_2H_6, Computed with BLYP and Four Different Basis Sets with All Electrons Treated Variationally, without (no CPC) and with Counterpoise Correction (with CPC).[b,c]

	RC		TS		P	
Basis set	no CPC	with CPC	no CPC	with CPC	no CPC	with CPC
ae-DZ	−4.2	−2.2	23.2	26.5	−5.5	−1.8
ae-TZP	−6.2	−6.1	19.7	20.0	−7.8	−7.2
ae-TZ2P	−6.7	−6.5	18.5	18.9	−9.5	−9.0
ae-QZ4P	−6.8	−6.8	18.0	18.0	−9.7	−9.6

[a]Geometries optimized at ZORA-BLYP/TZ2P with frozen-core approximation, see Figure 1.
[b]Relativistic effects treated with ZORA (see Method section).

much less delicate role of describing polarization of the electron density. In conclusion, the TZ2P basis in combination with the frozen-core approximation yields an efficient and accurate description of the relative energies of our stationary points.

Finally, based again on the ZORA-BLYP/TZ2P geometries discussed above, we have computed the relative energies of stationary points along the PES for various LDA, GGAs, meta-GGAs, and hybrid functionals in combination with the all-electron ae-TZ2P basis set and ZORA for relativistic effects. This was done in a post-SCF manner, that is, using density functionals with the electron density obtained at ZORA-BLYP/ae-TZ2P. The performance of the density functionals is discussed by comparing the resulting potential energy surfaces with that of the *ab initio* [CCSD(T)] benchmark discussed above. The results of this survey are collected in Table 8, which shows energies relative to the separate reactants (R). Energies relative to the reactant complex are summarized in Table 9 and will be discussed in the last subsection.

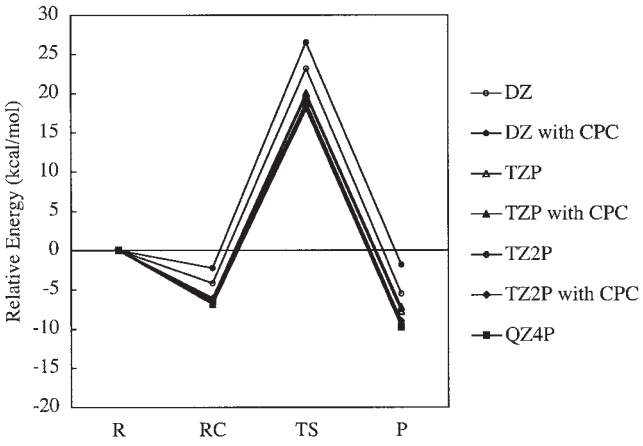

Figure 4. Reaction profile for the oxidative insertion of Pd into the C—C bond of C_2H_6, computed with ZORA-BLYP and four different basis sets with all electrons treated variationally, without (no CPC) and with counterpoise correction (with CPC). Based on geometries optimized at ZORA-BLYP/TZ2P (i.e., using the frozen-core approximation).

For clarity, we wish to point out that the above procedure for computing the relative energies shown in Table 8 differs in three respects from that used for computing the relative energies with the seven GGA functionals shown in Table 6: (1) an all-electron approach is used instead of the frozen-core approximation; (2) for all density functionals, the BLYP optimized geometries are used instead of geometries optimized with the same functional; and (3) for all functionals, the BLYP electron density is used for computing the energy instead of the electron density corresponding to that functional. The effect of going from frozen-core (TZ2P) to all-electron calculations (ae-TZ2P), that is, point (1), is negligible, causing a stabilization of 0.2 kcal/mol or less, and has already been discussed above. The differences between the values in Tables 6 and 8 derive mainly from the combined effects of points (2) and (3), which causes a destabilization of up to 1.7 (for the OLYP transition state) of the relative energies if one goes from Table 6 to Table 8. Both effects are in the order of a few tenths of a kcal/mol up to maximally 1 kcal/mol and, for the different GGA functionals and stationary points, contribute to this destabilization with varying relative importance. For the TS, the single-point approach contributes generally somewhat more (0.6–1.0 kcal/mol) to this destabilization than the post-SCF approach (0.1–0.4 kcal/mol, with an exceptionally high value of 0.8 kcal/mol for OLYP). This has been assessed by computing the relative energies of stationary points using approximation (2) but not (3), that is, computing them with the electron density corresponding to the density functional under consideration but with the BLYP geometries; the resulting values are provided in parentheses in Table 8. In conclusion, the combined effect of approximations (1)–(3) on the relative energies of stationary points is in the order of 1 kcal/mol, with an upper limit of 1.7 kcal/mol.

Now, we extend our survey to the full range of energy density functionals that, except for LDA and the seven GGAs discussed above, have been implemented in the ADF program in a post-SCF manner. For all 24 density functionals, we have computed the mean absolute error in the relative energies of reactant complex, transition state and product, and the error in the barrier, that is, the relative energy of the transition state, compared with the CCSD(T) benchmark (see Table 8). Both the mean absolute error and the error in the barrier drop significantly if one goes from LDA (mean abs. err. = 19.7 kcal/mol), which suffers from its infamous

Table 8. Energies (kcal/mol) Relative to the Separate Reactants (R) of the Stationary Points[a] along the Reaction Coordinate for Oxidative Insertion of Pd into the C—C Bond of C_2H_6, and Dissociation Energy of Ethane into Two Methyl Radicals (D_{CC}), Computed for 24 Different Density Functionals with the ae-TZ2P Basis Set with All Electrons Treated Variationally.[b]

Method	RC	TS	P	Mean abs. err. rel. to R[c]	Err. in barr. rel. to R[c]	D_{CC}	Err. in D_{CC}[d]
LDA							
VWN	−22.7 (−23.0)	−5.2 (−5.5)	−27.2 (−27.3)	19.7	−24.7	114.5	24.0
GGAs							
BP86	−10.4 (−10.4)	12.3 (12.1)	−13.3 (−13.4)	5.4	−7.1	93.0	2.5
BLYP	−6.7	18.5	−9.5	3.4	−0.9	90.0	−0.5
Becke88x + BR89c	−7.4	17.3	−11.6	4.2	−2.1	91.3	0.8
PW91	−11.8 (−11.8)	10.8 (10.7)	−14.1 (−14.0)	6.4	−8.6	96.2	5.7
PBE	−11.3 (−11.3)	11.5 (11.2)	−13.2 (−13.2)	5.7	−7.9	96.3	5.8
FT97	−11.9	12.2	−14.8	6.2	−7.2	93.5	3.0
revPBE	−6.2 (−6.3)	18.3 (17.9)	−7.6 (−7.6)	2.9	−1.1	90.5	0.0
HCTH/93	−1.0	27.2	2.4	8.2	7.8	91.2	0.7
RPBE	−5.7 (−5.8)	19.2 (18.8)	−6.7 (−6.8)	2.5	−0.2	89.9	−0.6
BOP	−3.5	22.7	−5.8	4.0	3.3	89.3	−1.2
HCTH/120	−5.4	21.7	−2.7	3.2	2.3	93.2	2.7
HCTH/147	−4.7	22.3	−2.2	3.7	2.9	93.2	2.7
HCTH/407	−2.6	26.9	2.5	7.6	7.5	91.6	1.1
OLYP	−0.5 (−1.1)	26.8 (26.0)	1.6 (1.1)	7.9	7.4	91.3	0.8
Meta-GGAs							
BLAP3	−0.8	29.9	0.3	8.4	10.5	91.8	1.3
VS98	−10.9	16.2	−5.8	1.5	−3.2	89.9	−0.6
KCIS	−8.3	13.6	−11.1	5.0	−5.8	91.7	1.2
PKZB	−6.8	15.2	−10.4	4.7	−4.2	89.8	−0.7
Bmτ1	−0.5	30.6	0.6	8.9	11.2	90.2	−0.3
OLAP3	5.5	38.3	11.5	17.0	18.9	93.1	2.6
TPSS	−8.6	14.8	−11.4	4.6	−4.6	90.3	−0.2
Hybrid functionals							
B3LYP(VWN5)	−4.9	25.2	0.2	5.4	5.8	90.4	−0.1
TPSSh	−7.3	18.6	−6.2	2.0	−0.8	90.1	−0.4

[a]Geometries optimized at ZORA-BLYP/TZ2P with frozen-core approximation, see Figure 1.
[b]Computed post-SCF using the BLYP electron density, unless stated otherwise. Values in parentheses computed self-consistently, that is, with the potential and electron-density corresponding to the energy functional indicated. Relativistic effects treated with ZORA (see Method section).
[c]Mean absolute error for the energies of the three stationary points RC, TS, and P relative to the separate reactants (R) and error in the overall barrier, that is, in the energy of the TS relative to R, compared with the CCSD(T) benchmark from this work.
[d]Error in the dissociation energy of the C—C bond in ethane, compared with CCSD(T) benchmark from this work, which amounts to 90.5 kcal/mol (see Results section).

overbinding, to GGA functionals (mean abs. err. = 2.5 to 8.2 kcal/mol). However, no significant improvement occurs if one goes from GGA to the more recently developed meta-GGA (mean abs. err. = 1.5–17.0 kcal/mol) and hybrid functionals (mean abs. err. = 2.0–5.4 kcal/mol). Best overall agreement with the *ab initio* benchmark PES is achieved by functionals of the GGA (RPBE), meta-GGA (VS98), as well as hybrid-DFT type (TPSSh), with mean absolute errors of 1.5 to 2.5 kcal/mol and errors in the barrier ranging from −3.3 to −0.3 kcal/mol. Interestingly, the well-known BLYP functional compares very reasonably with an only slightly larger mean absolute error of 3.4 kcal/mol and an underestimation of the barrier of only −0.9 kcal/mol. Apart from RPBE, only one other functional performs better in calculating the activation barrier, namely the TPSSh hybrid functional, with an underestimation of the barrier of only −0.8 kcal/mol. Note also that the widely used B3LYP hybrid functional does not perform better for this PES, with a significantly higher mean absolute error of 5.4 kcal/mol and an overestimation of the barrier by not less than 5.8 kcal/mol.

The above agrees with and further corroborates our previous finding for the Pd + methane system in which B3LYP was also found to perform slightly worse than BLYP.[25] Our results also nicely agree with experimental findings by Weisshaar and coworkers,[95] who already noted a general tendency in case of 3*d* transition metal ions, and in particular Co^+, for the B3LYP functional to overestimate reaction barrier heights for insertion

Table 9. Energies (in kcal/mol) Relative to the Reactant Complex (RC) of the Stationary Points[a] along the Reaction Coordinate for Oxidative Insertion of Pd into the C—C Bond of C_2H_6, Computed for 24 Different Density Functionals with the ae-TZ2P Basis Set with All Electrons Treated Variationally.[b]

Method	R	TS	P	Mean abs. err. rel. to RC[c]	Err. in barr. rel. to RC[c]
LDA					
VWN	22.7	17.5	−4.5	11.8	−12.7
GGAs					
BP86	10.4	22.7	−2.9	5.7	−7.5
BLYP	6.7	25.2	−2.8	6.1	−5.0
Becke88x + BR89c	7.4	24.7	−4.2	6.5	−5.5
PW91	11.8	22.6	−2.3	5.7	−7.6
PBE	11.3	22.8	−1.9	5.4	−7.4
FT97	11.9	24.1	−2.9	5.5	−6.1
revPBE	6.2	24.5	−1.4	6.0	−5.7
HCTH/93	1.0	28.2	3.4	4.9	−2.0
RPBE	5.7	24.9	−1.0	5.9	−5.3
BOP	3.5	26.2	−2.3	6.6	−4.0
HCTH/120	5.4	27.1	2.7	4.1	−3.1
HCTH/147	4.7	27.0	2.5	4.4	−3.2
HCTH/407	2.6	29.5	5.1	3.3	−0.7
OLYP	0.5	27.3	2.1	5.8	−2.9
Meta-GGAs					
BLAP3	0.8	30.7	1.1	5.2	0.5
VS98	10.9	27.1	5.1	1.5	−3.1
KCIS	8.3	21.9	−2.8	6.6	−8.3
PKZB	6.8	22.0	−3.6	7.4	−8.2
Bmτ1	0.5	31.1	1.1	5.5	0.9
OLAP3	−5.5	32.8	6.0	6.4	2.6
TPSS	8.6	23.4	−2.8	6.0	−6.8
Hybrid functionals					
B3LYP(VWN5)	4.9	30.1	5.1	2.4	−0.1
TPSSh	7.3	25.9	1.1	4.3	−4.3

[a]Geometries optimized at ZORA-BLYP/TZ2P with frozen-core approximation, see Figure 1.
[b]Computed post-SCF using the BLYP electron density. Relativistic effects treated with ZORA (see Method section).
[c]Mean absolute error for the relative energies of the three stationary points R, TS, and P relative to the reactant complex (RC) and error in the central barrier, in the energy of the TS relative to RC, compared with the CCSD(T) benchmark from this work.

in C—H and C—C bonds. They proved that, using a statistical rate model, B3LYP energies cannot fit experiment at all. However, adjusting the reaction barrier heights (relative to reactants) downward with 4–7 kcal/mol leads to good agreement with experiment. Independently, we reach the same result, namely that B3LYP overestimates the barrier (relative to reactants) by almost 6 kcal/mol.

Performance for the Central Barrier

So far, we have concentrated on the overall activation energy, that is, the difference in energy between the separate reactants which, as pointed out earlier, is decisive for the rate of chemical reactions in the gas phase, in particular, if they occur under low-pressure conditions in which the reaction system is (in good approximation) thermally isolated.[7,42,43] Here, we address the central barrier, that is, the difference in energy between the TS and the reactant complex. The latter becomes decisive in the high-pressure regime, when termolecular collisions are sufficiently efficient to cool the otherwise rovibrationally hot reactant complex, causing it to be in thermal equilibrium with the environment. In Table 9 we have collected the energies of the separate reactants (R), the transition state (TS), and the product (P) relative to the reactant complex (RC).

The mean absolute error changes by changing the point of reference from the separate reactants (in Table 8) to the reactant complex (in Table 9). Now, B3LYP (mean abs. err. = 2.4 kcal/mol) performs significantly better than BLYP (mean abs. err. = 6.1 kcal/mol) and is only surpassed by the performance of the GGA functional VS98 (mean abs. err. = 1.5 kcal/mol). Whereas BLYP is better for computing the overall barrier (i.e., TS relative to R), it is B3LYP that outperforms BLYP for the central barrier (i.e., TS relative to RC). We recall that BLYP underestimates the overall barrier by only −0.9 kcal/mol, whereas B3LYP overesti-

mates this barrier by 5.8 kcal/mol (see Table 8). The latter overestimation originates partially from the fact that B3LYP yields a too weakly bound reactant complex. Once this deficiency is switched off, by taking the reactant complex as the point of reference, B3LYP performs very well (see Table 9): it underestimates the barrier by only −0.1 kcal/mol, whereas BLYP underestimates the central barrier by −5.0 kcal/mol.

We have verified that errors made by BLYP or B3LYP in overall or central barriers do not originate from a failure in describing the C—C bond dissociation. To this end, we have first computed an *ab initio* benchmark for the C—C bond strength, that is, the dissociation energy D_{CC} associated with the reaction $H_3C—CH_3 \rightarrow 2\ CH_3\cdot$, at the same levels of theory as we did for the PES of the oxidative addition of the ethane C—C bond to Pd. This was done again using the BLYP-optimized geometries, which yield a C—H bond length of 1.084 Å for the D_{3h} symmetric methyl radical. Thus, we arrive at a dissociation energy of 90.5 kcal/mol at CCSD(T) (HF: 68.0, MP2: 94.0, and CCSD: 88.4 kcal/mol; for details, see Table S2 in the supplementary material), in nice agreement with previous findings (cf., e.g., Robertson and coworkers: 94.0[96] and 87.6 kcal/mol;[97] Lorant et al.: 95.8 kcal/mol[98]). Most functionals are able to describe the dissociation energy reasonably well, yielding errors, compared with the CCSD(T) benchmark, in the order of a kcal/mol or less. For BLYP and B3LYP, the dissociation energy D_{CC} is underestimated by only 0.5 and 0.1 kcal/mol, respectively (see Table 8). All together, we conclude that both BLYP and B3LYP are reasonable approaches for tackling the oxidative addition of the ethane C—C bond to palladium.

Conclusions

We have computed an *ab initio* benchmark for the archetypal oxidative addition of the ethane C—C bond to palladium that derives from a hierarchical series of relativistic methods and highly polarized basis sets for the palladium atom, up to the counterpoise corrected, four-component spin-free Dirac–Coulomb CCSD(T)/(24*s*16*p*13*d*+4*f*+*p*+*g*) level, which is converged with respect to the basis-set size within a few tenths of a kcal/mol. Our findings stress the importance of sufficient higher angular momentum polarization functions, *f* and *g*, as well as counterpoise correction for obtaining reliable activation energies.

This benchmark is used to evaluate the performance of 24 relativistic (ZORA) density functionals for describing geometries and relative energies of stationary points on the potential energy surface. Excellent agreement with our *ab initio* benchmark for energies relative to reactants, is achieved by functionals of the GGA, meta-GGA as well as hybrid DFT approaches, each of which have a representative in the top three, with mean absolute errors as small as 2.5 kcal/mol or less. Neither hybrid DFT nor the meta-GGA represents a systematic improvement over GGA functionals. Interestingly, the well-known BLYP functional still performs satisfactorily with mean absolute errors of 3.4 and 6.1 kcal/mol for energies relative to reactants and reactant complex, respectively, and an underestimation of the overall barrier (i.e., TS relative to reactants) by only −0.9 kcal/mol and of the central barrier (i.e., TS relative to reactant complex) by −5.0 kcal/mol. Note that the much advocated B3LYP hybrid functional also performs well, but not significantly better than BLYP, with mean absolute errors of 5.4 and 2.4 kcal/mol for energies relative to reactants and reactant complex, respectively, and an overestimation of the overall barrier by 5.8 kcal/mol and an underestimation of the central barrier by only −0.1 kcal/mol. These results parallel our previous finding for the oxidative addition of CH_4 + Pd.[25]

Our results have been verified to be converged with the basis-set size at ZORA-BLYP/TZ2P and to be unaffected by the frozen-core approximation for the core shells of carbon (1*s*), chlorine (1*s*2*s*2*p*), and palladium (1*s*2*s*2*p*3*s*3*p*3*d*). We consider this a sound and efficient approach for the routine investigation of catalytic bond activation, also in larger, more realistic model systems.

Acknowledgments

We thank Dr. L. Visscher, Dr. J. N. P. van Stralen and I. Infante for helpful discussions. We thank the staff of the Stichting Academisch Rekencentrum Amsterdam (SARA) for their generous assistance.

References

1. Shilov, A. E.; Shul'pin, G. B. Chem Rev 1997, 97, 2879.
2. Crabtree, R. H. Chem Rev 1995, 95, 987.
3. Arndtsen, B. A.; Bergman, R. G.; Mobley, T. A.; Peterson, Th. H. Acc Chem Res 1995, 28, 154.
4. Dedieu, A. Chem Rev 2000, 100, 543.
5. Fayet, P.; Kaldor, A.; Cox, D. M. J Chem Phys 1990, 92, 254.
6. Weisshaar, J. C. Acc Chem Res 1993, 26, 213.
7. Carroll, J. J.; Weisshaar, J. C. J Am Chem Soc 1993, 115, 800.
8. Carroll, J. J.; Haug, K. L.; Weisshaar, J. C.; Blomberg, M. R. A.; Siegbahn, P. E. M.; Svensson, M. J Phys Chem 1995, 99, 13955.
9. Campbell, M. L. Chem Phys Lett 2002, 365, 361.
10. Low, J. J.; Goddard, W. A., III. J Am Chem Soc 1984, 106, 8321.
11. Low, J. J.; Goddard, W. A., III. Organometallics 1986, 5, 609.
12. Blomberg, M. R. A.; Siegbahn, P. E. M.; Nagashima, U.; Wennerberg, J. J Am Chem Soc 1991, 113, 424.
13. Svensson, M.; Blomberg, M. R. A.; Siegbahn, P. E. M. J Am Chem Soc 1991, 113, 7076.
14. Blomberg, M. R. A.; Siegbahn, P. E. M.; Svensson, M. J Am Chem Soc 1992, 114, 6095.
15. Siegbahn, P. E. M.; Blomberg, M. R. A. J Am Chem Soc 1992, 114, 10548.
16. Siegbahn, P. E. M.; Blomberg, M. R. A.; Svensson, M. J Am Chem Soc 1993, 115, 1952.
17. Heiberg, H.; Gropen, O.; Swang, O. Int J Quantum Chem 2003, 92, 391.
18. Wittborn, A. M. C.; Costas, M.; Blomberg, M. R. A.; Siegbahn, P. E. M. J Chem Phys 1997, 107, 4318.
19. Diefenbach, A.; Bickelhaupt, F. M. J Chem Phys 2001, 115, 4030.
20. de Jong, G. Th.; Visscher, L. Theor Chem Acc 2002, 107, 304.
21. Smurnyi, E. D.; Gloriozov, I. P.; Ustynuk, Yu. A. Russ J Phys Chem 2003, 77, 1699.
22. Jun, C. H. Chem Soc Rev 2004, 33, 610.
23. Diefenbach, A.; Bickelhaupt, F. M. J Phys Chem A 2004, 108, 8460.
24. de Jong, G. Th.; Solà, M.; Visscher, L.; Bickelhaupt, F. M. J Chem Phys 2004, 121, 9982.

25. de Jong, G. Th.; Geerke, D. P.; Diefenbach, A.; Bickelhaupt, F. M. Chem Phys 2005, 313, 261.
26. Hohenberg, P.; Kohn, W. Phys Rev 1964, 136, B864.
27. Kohn, W.; Sham, L. J. Phys Rev 1965, 140, A1133.
28. Parr, R. G.; Yang, W. Density-Functional Theory of Atoms and Molecules; Oxford University Press: New York, 1989.
29. Møller, C; Plesset, M. S. Phys Rev 1934, 46, 618.
30. Cizek, J. J Chem Phys 1966, 45, 4256.
31. Purvis, G. D., III.; Bartlett, R. J. J Chem Phys 1982, 76, 1910.
32. Raghavachari, K.; Trucks, G. W.; Pople, J. A.; Head–Gordon, M. Chem Phys Lett 1989, 157, 479.
33. Boys, S. F.; Bernardi, F. Mol Phys 1970, 19, 553.
34. Siegbahn, P. E. M.; Blomberg, M. R. A.; Svensson, M. Chem Phys Lett 1994, 223, 35.
35. Diefenbach, A.; de Jong, G. Th.; Bickelhaupt, F. M. Mol Phys 2005, 103, 995.
36. Baker, J.; Muir, M.; Andzelm, J. J Chem Phys 1995, 102, 2063.
37. Barone, V.; Adamo, C. J Chem Phys 1996, 105, 11007.
38. Thümmel, H. T.; Bauschlicher, C. W., Jr. J Phys Chem A 1997, 101, 1188.
39. Bach, R. D.; Glukhovtsev, M. N.; Gonzales, C. J Am Chem Soc 1998, 120, 9902.
40. Gritsenko, O. V.; Ensing, B.; Schippers, P. R. T.; Baerends, E. J. J Phys Chem A 2000, 104, 8558.
41. Poater, J. Phys Chem Chem Phys 2002, 4, 722.
42. Nibbering, N. M. M. Adv Phys Org Chem 1988, 24, 1.
43. Bickelhaupt, F. M. Mass Spectrom Rev 2001, 20, 347.
44. Baerends, E. J.; Ellis, D. E.; Ros, P. Chem Phys 1973, 2, 41.
45. Fonseca Guerra, C.; Snijders, J. G.; te Velde, G.; Baerends, E. J. Theor Chem Acc 1998, 99, 391.
46. te Velde, G.; Bickelhaupt, F. M.; Baerends, E. J.; Fonseca Guerra, C.; van Gisbergen, S. J. A.; Snijders, J. G.; Ziegler, T. J Comput Chem 2001, 22, 931.
47. Baerends, E. J.; Autschbach, J. A.; Bérces, A.; Bo, C.; Boerrigter, P. M.; Cavallo, L.; Chong, D. P.; Deng, L.; Dickson, R. M.; Ellis, D. E.; Fan, L.; Fischer, T. H.; Fonseca Guerra, C.; van Gisbergen, S. J. A.; Groeneveld, J. A.; Gritsenko, O. V.; Grüning, M.; Harris, F. E.; van den Hoek, P.; Jacobsen, H.; van Kessel, G.; Kootstra, F.; van Lenthe, E.; Osinga, V. P.; Patchkovskii, S.; Philipsen, P. H. T.; Post, D.; Pye, C. C.; Ravenek, W.; Ros, P.; Schipper, P. R. T.; Schreckenbach, G.; Snijders, J. G.; Sola, M.; Swart, M.; Swerhone, D.; te Velde, G.; Vernooijs, P.; Versluis, L.; Visser, O.; van Wezenbeek, E.; Wiesenekker, G.; Wolff, S. K.; Woo, T. K.; Ziegler, T. Computer code ADF2002.03; SCM, Theoretical Chemistry, Vrije Universiteit: Amsterdam, The Netherlands, 2002.
48. Becke, A. D. Phys Rev A 1988, 38, 3098.
49. Perdew, J. P. Phys Rev B 1986, 33, 8822.
50. Lee, C.; Yang, W.; Parr, R. G. Phys Rev B 1988, 37, 785.
51. Perdew, J. P. In Electronic Structure of Solids '91; Ziesche, P.; Eschrig, H., Eds.; Akademie Verlag: Berlin, 1991.
52. Perdew, J. P.; Wang, Y. Phys Rev B 1992, 45, 13244.
53. Perdew, J. P.; Chevary, J. A.; Vosko, S. H.; Jackson, K. A.; Pederson, M. R.; Singh, D. J.; Fiolhais, C. Phys Rev B 1992, 46, 6671.
54. Perdew, J. P.; Chevary, J. A.; Vosko, S. H.; Jackson, K. A.; Pederson, M. R.; Singh, D. J.; Fiolhais, C. Phys Rev B 1993, 49, 4978(E).
55. Perdew, J. P.; Burke, K.; Ernzerhof, M. Phys Rev Lett 1996, 77, 3865.
56. Perdew, J. P.; Burke, K.; Ernzerhof, M. Phys Rev Lett 1997, 78, 1396(E).
57. Zhang, Y.; Yang, W. Phys Rev Lett 1998, 80, 890.
58. Hammer, B.; Hansen, L. B.; Nørkov, J. K. Phys Rev B 1999, 59, 7413.
59. Handy, N. C.; Cohen, A. J. Mol Phys 2001, 99, 403.
60. van Lenthe, E.; Baerends, E. J.; Snijders, J. G. J Chem Phys 1994, 101, 9783.
61. Visscher, L.; Lee, T. J.; Dyall, K. G. J Chem Phys 1996, 105, 8769.
62. Jensen, H. J. Aa.; Saue, T.; Visscher, L. Computer Code DIRAC, release 4.0; Syddansk Universitet: Odense, Denmark, 2004.
63. Dyall, K. G. J Chem Phys 1994, 100, 2118.
64. Visscher, L. Theor Chem Acc 1997, 98, 68.
65. Dunning, Th. H., Jr. J Chem Phys 1989, 90, 1007.
66. Kendall, R. A.; Dunning, Th. H., Jr.; Harrison, R. J. J Chem Phys 1992, 96, 6796.
67. Visscher, L.; Aerts, P. J. C.; Visser, O.; Nieuwpoort, W. C. Int J Quantum Chem: Quantum Chem Symp 1991, 25, 131.
68. Ehlers, A. W.; Böhme, M.; Dapprich, S.; Gobbi, A.; Höllwarth, A.; Jonas, V.; Köhler, K. F.; Stegmann, R.; Veldkamp, A.; Frenking, G. Chem Phys Lett 1993, 208, 111.
69. Langhoff, S. R.; Petterson, L. G. M.; Bauschlicher, C. W., Jr. J Chem Phys 1987, 86, 268.
70. Osanai, Y.; Sekiya, M.; Noro, T.; Koga, T. Mol Phys 2003, 101, 65.
71. Vosko, S. H.; Wilk, L.; Nusair, M. Can J Phys 1980, 58, 1200.
72. Becke, A. D. J Chem Phys 1988, 88, 1053.
73. Becke, A. D.; Roussel, M. R. Phys Rev A 1989, 39, 3761.
74. Filatov, M.; Thiel, W. Mol Phys 1997, 91, 847.
75. Hamprecht, F. A.; Cohen, A. J.; Tozer, D. J.; Handy, N. C. J Chem Phys 1998, 109, 6264.
76. Tsuneda, T.; Suzumura, T.; Hirao, K. J Chem Phys 1999, 110, 10664.
77. Boese, A. D.; Doltsinis, N. L.; Handy, N. C.; Sprik, M. J Chem Phys 2000, 112, 1670.
78. Boese, A. D.; Handy, N. C. J Chem Phys 2001, 114, 5497.
79. Proynov, E. I.; Sirois, S.; Salahub, D. R. Int J Quantum Chem 1997, 64, 427.
80. van Voorhis, T.; Scuseria, G. E. J Chem Phys 1998, 109, 400.
81. Krieger, J. B.; Chen, J.; Iafrate, G. J.; Savin, A. In Electron Correlation and Material Properties; Gonis, A.; Kioussis, N., Eds.; Plenum: New York, 1999.
82. Perdew, J. P.; Kurth, S.; Zupan, A.; Blaha, P. Phys Rev Lett 1999, 82, 2544.
83. Perdew, J. P.; Kurth, S.; Zupan, A.; Blaha, P. Phys Rev Lett 1999, 82, 5179(E).
84. Proynov, E.; Chermette, H.; Salahub, D. R. J Chem Phys 2000, 113, 10013.
85. Tao, J.; Perdew, J. P.; Staroverov, V. N.; Scuseria, G. E. Phys Rev Lett 2003, 91, 146401.
86. Staroverov, V. N.; Scuseria, G. E.; Tao, J.; Perdew, J. P. J Chem Phys 2003, 119, 12129.
87. Becke, A. D. J Chem Phys 1993, 98, 5648.
88. Stephens, P. J.; Devlin, F. J.; Chabalowski, C. F.; Frisch, M. J. J Phys Chem 1994, 98, 11623.
89. Hertwig, R. H.; Koch, W. Chem Phys Lett 1997, 268, 345.
90. Frenking, G.; Antes, I.; Böhme, M.; Dapprich, S.; Ehlers, A. W.; Jonas, V.; Neuhaus, A.; Otto, M.; Stegmann, R.; Veldkamp, A.; Vyboishchikov, S. F. In Reviews in Computational Chemistry; Lipkowitz, K. B.; Boyd, D. B., Eds.; VCH Publishers Inc.: New York, 1996, p. 63.
91. Cundari, Th. R.; Benson, M. T.; Lutz, M. L. In Reviews in Computational Chemistry; Lipkowitz, K. B.; Boyd, D. B., Eds.; VCH Publishers Inc.: New York, 1996, p. 145.
92. Hay, P. J.; Wadt, W. R. J Chem Phys 1985, 82, 299.
93. Jonas, V.; Frenking, G.; Reetz, M. T. J Comput Chem 1992, 13, 919.
94. Frisch, M. J.; Trucks, G. W.; Schlegel, H. B.; Scuseria, G. E.; Robb, M. A.; Cheeseman, J. R.; Montgomery, Jr., J. A.; Vreven, T.; Kudin, K. N.; Burant, J. C.; Millam, J. M.; Iyengar, S. S.; Tomasi, J.; Barone, V.; Mennucci, B.; Cossi, M.; Scalmani, G.; Rega, N.; Petersson,

G. A.; Nakatsuji, H.; Hada, M.; Ehara, M.; Toyota, K.; Fukuda, R.; Hasegawa, J.; Ishida, M.; Nakajima, T.; Honda, Y.; Kitao, O.; Nakai, H.; Klene, M.; Li, X.; Knox, J. E.; Hratchian, H. P.; Cross, J. B.; Bakken, V.; Adamo, C.; Jaramillo, J.; Gomperts, R.; Stratmann, R. E.; Yazyev, O.; Austin, A. J.; Cammi, R.; Pomelli, C.; Ochterski, J. W.; Ayala, P. Y.; Morokuma, K.; Voth, G. A.; Salvador, P.; Dannenberg, J. J.; Zakrzewski, V. G.; Dapprich, S.; Daniels, A. D.; Strain, M. C.; Farkas, O.; Malick, D. K.; Rabuck, A. D.; Raghavachari, K.; Foresman, J. B.; Ortiz, J. V.; Cui, Q.; Baboul, A. G.; Clifford, S.; Cioslowski, J.; Stefanov, B. B.; Liu, G.; Liashenko, A.; Piskorz, P.; Komaromi, I.; Martin, R. L.; Fox, D. J.; Keith, T.; Al-Laham, M. A.; Peng, C. Y.; Nanayakkara, A.; Challacombe, M.; Gill, P. M. W.; Johnson, B.; Chen, W.; Wong, M. W.; Gonzalez, C.; Pople, J. A. Computer Code Gaussian 03, Rev. A.11; Gaussian, Inc.: Pittsburgh, PA, 2003.

95. Yi, S. S.; Reichert, E. L.; Holthausen, M. C.; Koch, W.; Weisshaar, J. C. Chem Eur J 2000, 6.
96. Robertson, S. H.; Wardlaw, D. M.; Hirst, D. M. J Chem Phys 1993, 99, 7748.
97. Pesa, M.; Pilling, M. J.; Robertson, S. H. J Phys Chem A 1998, 102, 8526.
98. Lorant, F.; Behar, F.; Goddard, W. A., III; Tang, Y. J Phys Chem A 2001, 105, 7896.
99. Hay, P. J. J Am Chem Soc 1981, 103, 1390.
100. Huzinaga, S. J Chem Phys 1977, 66, 4245.
101. Raffenetti, R. C. J Chem Phys 1973, 58, 4452.